Advances in Science and Technology Research Journal, 2026, 20(1), 236–258 https://doi.org/10.12913/22998624/210134 ISSN 2299-8624, License CC-BY 4.0

Analysis of the influence of heat treatment of NC11LV steel on the durability and improvement of tools for ceramic roof tile strand forming by extrusion

Jan Marzec^{1,2}, Marek Robert Hawryluk^{1*}, Marzena Małgorzata Lachowicz¹, Tadeusz Leśniewski¹, Konrad Kamil Perzyński³

- ¹ Wrocław University of Science and Technology, Wybrzeże Stanisława Wyspiańskiego 27, 50-370 Wrocław, Poland
- ² Röben Polska Sp. z o.o. i Wspólnicy Sp. K., Ceramiczna 2, 55-300 Środa Śląska, Poland
- ³ AGH University of Science and Technology, al. Adama Mickiewicza 30, 30-059 Kraków, Poland
- * Corresponding author's e-mail: marek.hawryluk@pwr.edu.pl

ABSTARCT

This study presents the results of comprehensive research on the analysis of tool operation in the extrusion process of clay mass used for ceramic roof tile production. The aim of the research is to identify the key factors influencing tool wear and to indicate effective methods for increasing operational durability. The research showed that parameters such as pressure and temperature of the ceramic mass flow, containing hard mineral components, significantly influence the intensity of tool wear. The composition analysis of the ceramic mass indicated the presence of high-hardness fractions, including quartz, basalt, and albite. The occurrence of these components leads to accelerated abrasive wear of the tool working surfaces, creating a challenge for the efficiency and cost of the production process. The study included a comparison of several heat treatment variants of NC11LV tool steel. This enabled the selection of appropriate heat treatment parameters and the achievement of favorable mechanical properties, combining high hardness with resistance to brittle fracture and abrasion. These results were confirmed through both laboratory abrasive wear tests and operational conditions. For a more in-depth analysis of the process, advanced numerical modeling methods were applied. Particularly effective was the smoothed particle hydrodynamics (SPH) method, which allowed for accurate representation of complex flow phenomena of ceramic mass containing hard inclusions. The method enabled precise prediction of local stresses, flow paths, and tool wear intensity.

Keywords: abrasive wear, tool steel NC11LV, heat treatment, ceramic mass strand forming, smoothed particle hydrodynamics simulation.

INTRODUCTION

Ceramic tiles are one of the most common types of roofing materials. Due to the continuously increasing market demand, a significant portion of development efforts in the ceramic industry focuses on ensuring high production efficiency while addressing environmental protection and waste recycling issues [1–4]. Despite the implementation of modern technical solutions in the ceramic industry, the production process of ceramic roof tiles can still be divided into several standard stages. These include: raw

material extraction, body preparation, body storage, shaping of semi-finished products, drying of semi-finished products, coating (engobing), firing of finished products, and quality control at various stages of the process [5]. The most important stage of the process is the forming of the plastic ceramic mass. The diagram shown in Figure 1 illustrates the forming process starting from the dosing of the ceramic mass from storage. The material is then subjected to final grinding, mixing, and homogenization with the addition of water. The prepared mass is preliminarily shaped and extruded into a continuous band, which is

Received: 2025.07.28

Accepted: 2025.10.01

Published: 2025.11.21

subsequently cut to a specified length and finally formed using a stamping press.

The ceramic mass used for roof tiles production mainly contains clay raw materials, which, when combined with water, constitute the plastic component [6, 7]. In addition, quartz sand and ground production waste (ceramic) with additives (basalt grit) are added to the mass [8, 9]. These components act as non-plastic additives that reduce the plasticity of the mass and ensure the desired shrinkage during drying and firing [10]. Due to the abrasive nature of the formed mass, the parts of forming machines must exhibit high wear resistance [11]. A wide range of materials are used for wear protection in the ceramic industry, which can include: wear-resistant steels (Hardox), cold working tool steels (NC10, NC11LV) [12, 13]. Various durability-enhancing methods are also commonly applied, such as heat treatment, thermo-chemical treatment, and hardfacing [14]. The selection of an appropriate material and durability-enhancement method depends on the specific operating conditions of the given component. The selection of the appropriate material and the method of increasing their durability depends on the specific work of the component. Forming tools, which are responsible for shaping the material during the extrusion of the strip, are particularly exposed to wear. The primary wear mechanisms include abrasion, sometimes combined with corrosion, which accelerates material degradation [15-17]. Analyses indicate that coldwork tool steels are increasingly used for this application, particularly the NC11LV grade, whose properties allow for precise adjustment of the heat treatment process. As a result, high hardness is achieved, which ensures adequate wear resistance [18]. These properties are primarily due to the high chromium content of this steel grade. The shape, size, and distribution of carbides in the microstructure also play a significant role in determining wear resistance. The most common type of carbide is M₂C₃[19, 20] The proper selection of material and design of forming tools requires a lot of analysis and research work. Laboratory methods are used to evaluate hardness and resistance to abrasive wear. Equally important is a thorough understanding of the causes of intensive wear of machine components in the roof tile extrusion process. In this context, determining the composition of the formed mass is essential, with particular attention to the identification of hard fractions and analysis of the parameters registered during the process. However, accurate examination of certain phenomena and parameters under industrial conditions is difficult, and in some cases impossible. Therefore, recently, analysis supported by numerical modeling has been increasingly used in various industries for process design and analysis. [21, 22]. In the ceramic industry, however, this method is still relatively rarely used, mainly due to the complexity of modeling the formed material (clay with additives) [23]. A proper and comprehensive approach to this issue can streamline and simplify the analysis of the extrusion process for ceramic roof tiles [24]. The insights gained enable the development of solutions aimed at extending tool life and optimizing the forming process. Continued research and development in this area may contribute to innovative solutions that further modernize the ceramic industry and support its sustainable development.

MATERIALS AND METHODS

The research focused on improving the durability and identifying the causes of excessive wear of the forming tools used in the extrusion of ceramic roof tiles. These tools shape the product at an early stage, closely replicating the roof tile's form and ensuring the required thickness.

Work to extend service life focused on material optimization. Cold work tool steels,

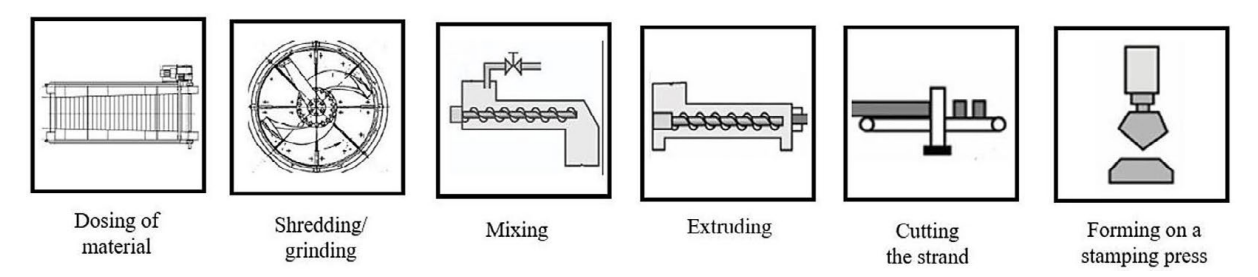


Figure 1. Diagram of the ceramic roof tile forming process

particularly the NC11LV grade, are increasingly used for forming tools. Accordingly, three heat treatment variants of this steel were subjected to laboratory and operational testing:

- Sample 960/450 Steel NC11LV hardening: 960 °C, tempering: 450 °C for 2 h;
- Sample 1060/450 Steel NC11LV hardening: 1060 °C, tempering: 450 °C for 2 h;
- Sample 1020/200 Steel NC11LV hardening: 1020 °C, tempering: 200 °C for 2 h.

The heat treatment of the individual test tools was carried out under controlled conditions in a vacuum furnace, following the process sequence outlined below:

- Stage 1: heating to 450 °C at a rate of 5 °C/min, holding for 20 min after temperature equalization;
- Stage 2: heating to 800 °C at a rate of 4 °C/min, holding for 20 min after temperature equalization;
- Stage 3: heating to the austenitizing temperature: 960 °C (sample 960/450), 1060 °C (sample 1060/450), 1020 °C (sample 1020/200), at a rate of 5 °C/min;
- Stage 4: holding at the austenitizing temperature for 20 min after complete temperature equalization;
- Stage 5: cooling vacuum atmosphere with N₂ gas at 6–10 bar and intensive flow. Cooling rate of 2.0 °C/s in the range of 800–500 °C. Cool to 50–70 °C, followed by immediate tempering;
- Stage 6: heating sample 960/450: 3 × 450 °C, 2 h each cycle; sample 1060/450: 3 × 450 °C, 2 h each cycle; sample 1020/200: 3 × 200 °C, 2 h each cycle.

In this study, NC11LV steel was subjected to three heat treatment variants. The treatment conditions were selected to assess their effect on the mechanical properties of this steel grade, with particular emphasis on abrasive wear resistance and impact toughness. The heat treatment of tool steel influences microstructure changes, particularly the number and size of carbide precipitates. This determines the key parameters for forming tools, which are: abrasion resistance, hardness and impact strength. Hardness, a key parameter for wear resistance, should be maximized and maintained at a stable level in tool steels. However, this typically comes at the expense of ductility, which increases the risk of cracking. Tempering at 450 °C

was implemented to achieve a balance between maintaining high hardness and improving ductility. To further validate the heat treatment conditions, two austenitizing temperatures were used: 960 °C and 1060 °C. This was verified by hardening the NC11LV steel at 1020 °C and tempering at 200 °C, which should ensure the highest hardness. The conducted research focused on verifying the knowledge regarding the heat treatment of NC11LV tool steel. For this purpose, its industrial application in the forming tools for ceramic roof tiles was used [18, 25, 26].

The following methods were used to verify tool wear and analyze the causes of degradation of tool materials:

- Verification of process parameters: pressure and temperature;
- SEM-EDS analysis of the formed material;
- Thermogravimetric analysis of the formed material;
- 3D scanning technique for worn forming tools;
- Dry abrasive wear test;
- Microstructure analysis;
- Hardness measurement.

Further analysis of the band extrusion process was carried out using numerical modeling. Based on the developed model in the Abaqus software, numerical simulations were performed to assess the potential for optimizing the forming tools through modifications in their design and geometry.

RESEARCH AND RESULTS DISCUSSION

Forming tool analysis

The forming tool ensures the desired shape, quality, and thickness of the extruded band. It is mounted at the end of the screw press and is a key part of the forming set. A typical forming tool is shown in Figure 2, it consists of two parts: upper and lower. This design allows for adjustment in case of wear.

The geometry of the tool ensures accurate filling of the die during the subsequent technological process, i.e., pressing on the stamp press. The produced band, with a specified width, provides a sufficient amount of flash during the forming operation in the punch press. Due to the direct contact of the tool with the formed material, it must primarily exhibit good wear resistance to ensure high durability and dimensional-shape

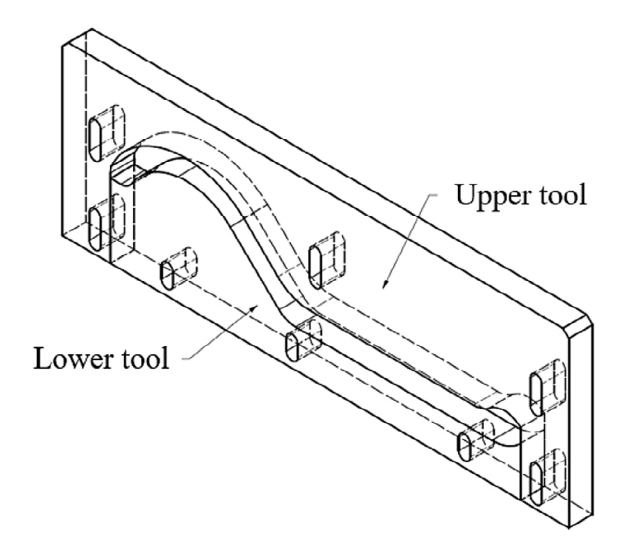


Figure 2. Roof tile forming tool diagram

repeatability. To meet these requirements, extensive testing and analysis are essential.

Analysis of the causes of wear

A lot of information about the cause of intensive wear of forming tools can be provided by a thorough verification of the forming process parameters, which show what loads the tools are exposed to during operation. In addition, an indepth analysis of the formed material is essential, as it is one of the primary factors contributing to abrasive wear.

Analysis of the parameters of the strand extrusion process

The extrusion process parameters are crucial for the operation of forming tools used in ceramic tile production. One of the key parameters in this process is the extrusion pressure, which is strictly defined, continuously monitored, and regulated. This pressure is generated in the chamber of the conical head. A schematic of the forming process in the conical head, including the location of pressure and temperature measurements, is shown in Figure 3.

The extrusion pressure should oscillate between 2.0–2.1 MPa during the production of ceramic tiles. In the analyzed process, the recording of this parameter was carried out on a screw press that produces two bands. Data were collected for 8 hours of operation and are shown in Figure 4

The analyzed operational period illustrates the variability of extrusion pressure during a single production shift. The chart shows that the pressure in the examined process remained at a level considered optimal for this type of operation. Observed pressure fluctuations are mainly due to variations in the moisture content of the extruded ceramic mass. Pressure regulation is achieved by controlled dosing of water into the screw press when pressure increases, the appropriate amount of added water reduces it to the desired level. Pressure drops below 1.5 MPa observed on the chart correspond to machine stoppages related to the need for tooling changeover.

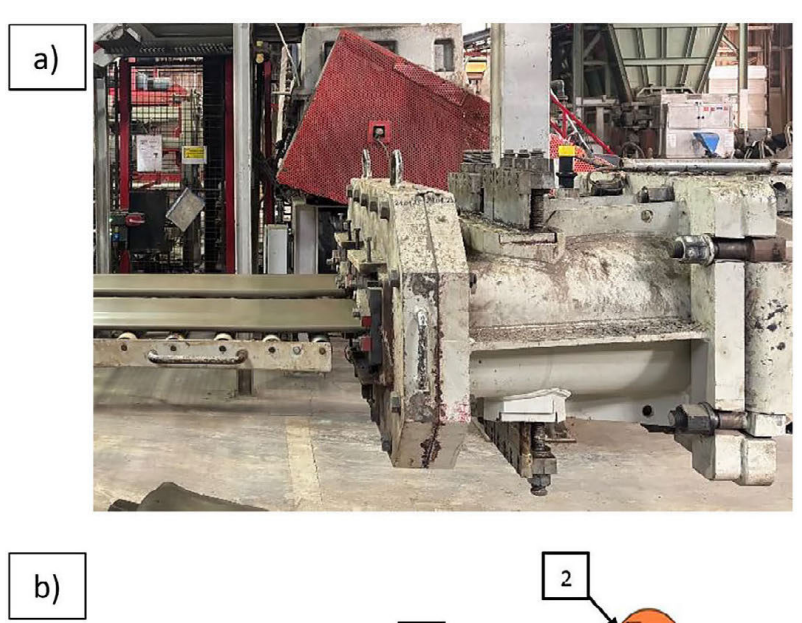
It is important to note that extrusion pressure directly influences other key parameters of the ceramic tile forming process, such as the temperature in the chamber of the conical head. This relationship is illustrated in the graph shown in Figure 5.

As shown in the chart (Figure 5), the temperature during the extrusion process remains around 45 °C. Analysis of the relationship between temperature and pressure showed that temperature drops are correlated with periods of machine stopped, suggesting a significant effect of process intensity on heat generation. The source of heat in the process in question is primarily friction both between the extruded mass and the working elements of the machine, as well as internal friction in the ceramic mass itself, resulting from the mutual sliding of its particles. This phenomenon is a key factor affecting the forming process and should be considered in process optimization.

SEM-EDS analysis of the formed mass

Accurate identification of the composition of the mass for the production of ceramic tiles is the basis for correct identification of the causes of wear of machine components in the forming process. This is primarily due to the abrasive nature of the material. A typical mass for the production of building ceramics consists of three basic groups of components: plastic materials, non-plastic and fluxes. For a detailed analysis of the production body, the most effective method is SEM-EDS analysis. The research was conducted on samples of standard mass taken directly from the production line.

In the image of the mass used for ceramic roof tile production shown in Figure 6, the main mineral fractions present in the material were identified. These include primarily: apatite, muscovite, quartz, albite, and biotite. Of particular importance in relation to the wear of forming tools are the hard mineral fractions contained



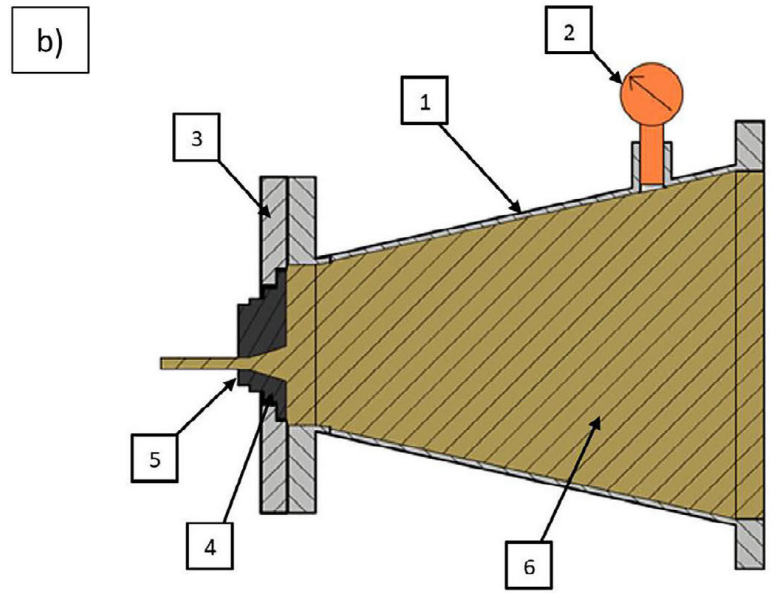


Figure 3. Production of ceramic roof tile: a) clay extrusion process, b) diagram of pressure head with sensor: 1-pressre head, 2-sensor, 3- assembling plate, 4-nozzle, 5-forming tool, 6-forming mass

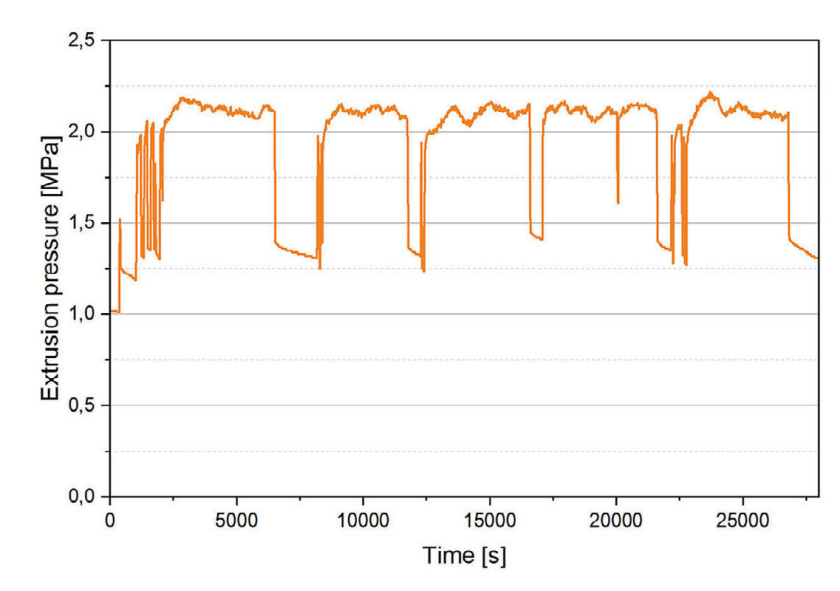


Figure 4. Graph of the strand extrusion pressure

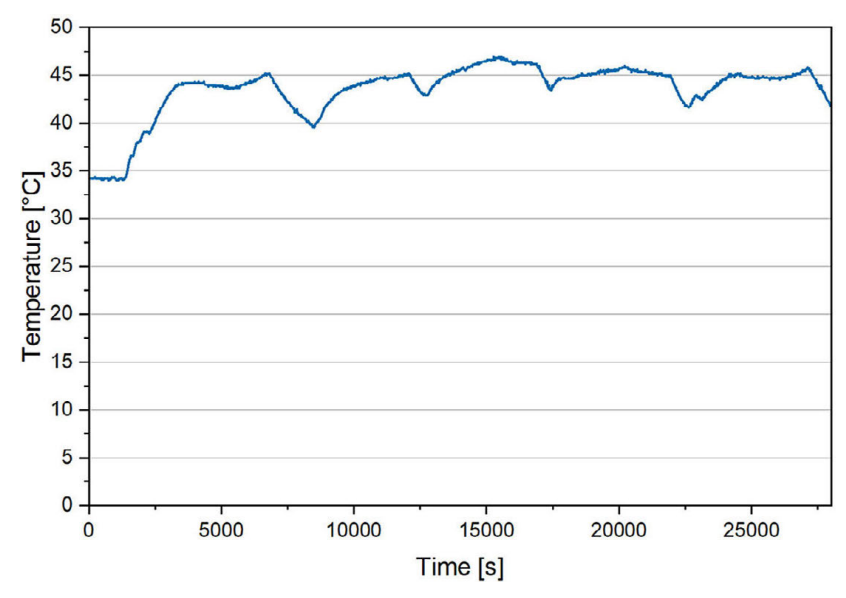


Figure 5. Graph of temperature inside pressure head during extrusiom ceramic roof tile

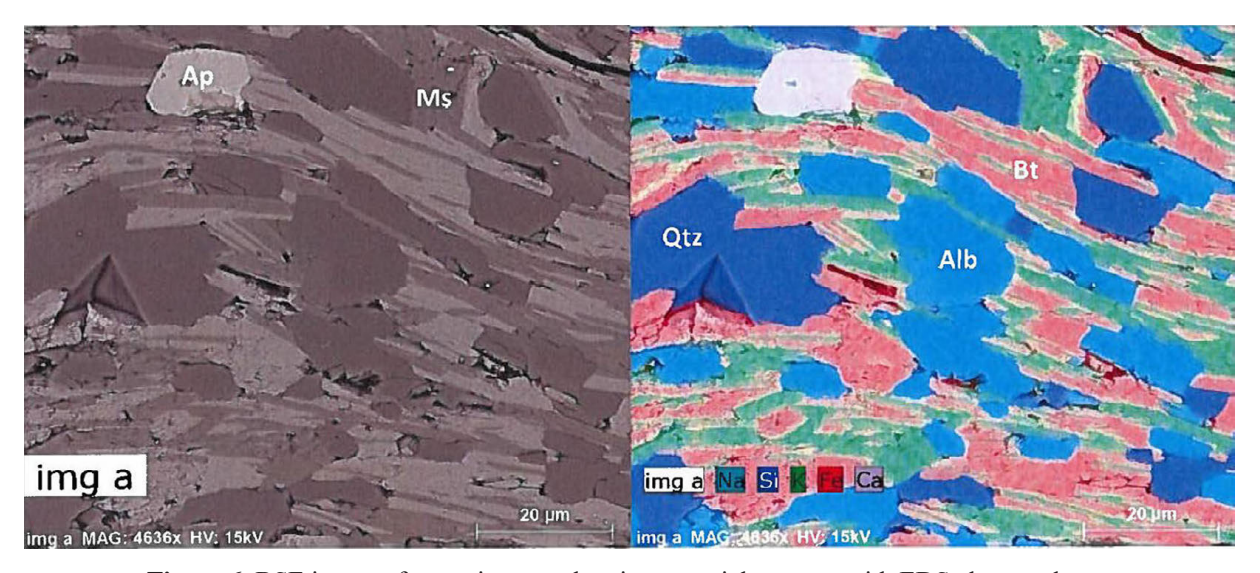


Figure 6. BSE image of ceramic mass showing material contrast with EDS elemental map

in the clay body. Among those identified in Figure 6, quartz and albite are especially relevant. A more detailed identification of these phases is presented in the BSE images combined with EDS spectra shown in Figure 7.

Quartz (Figure 7a) is characterized by high hardness, which is 7 on the Mohs scale. Harder mineral fractions also include albite (Figure 7b), with a hardness of 6–6.5 on the Mohs scale. Particularly abrasive wear is intensified by quartz, which is an abrasive mineral and is found in large quantities in clay tile mass. In the case of albite, its mineral grains can microscopically scratch and abrade steel surfaces, particularly during prolonged contact or abrasive motion. Although this

wear is not as aggressive as that caused by quartz, it may still result in gradual dulling, micro-damage, or surface degradation over time.

Further detailed analysis identified the presence of additional hard mineral fractions that contribute to the degradation of machine components, including the tools used for forming ceramic roof tiles. The identified minerals are presented in Figure 8.

Figure 8 shows an identified fragment of basalt, which constitutes one of the non-plastic additives in the composition of the ceramic body. Basalt is characterized by high hardness, reaching 8.5 on the Mohs scale, which significantly exceeds the hardness of typical tool materials. Therefore, it is an important component of the

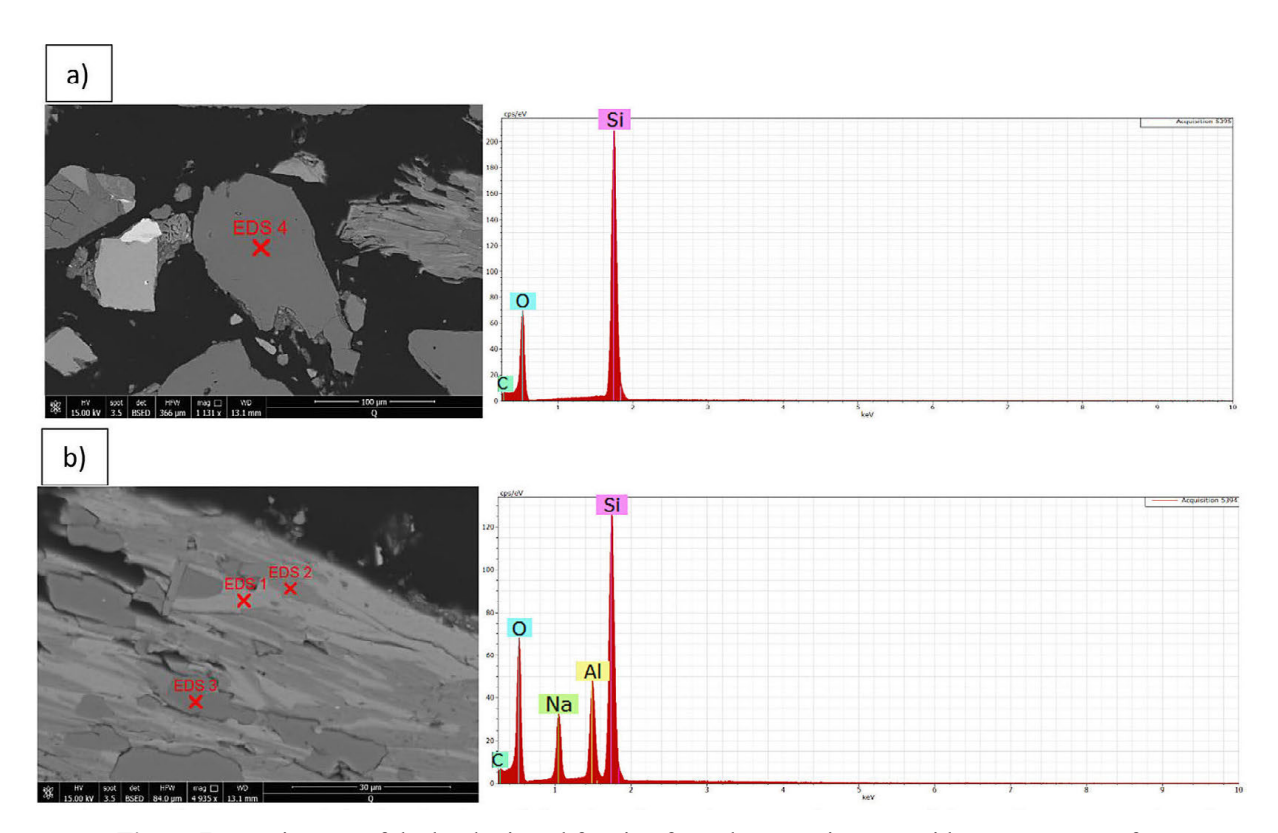


Figure 7. BSE images of the hard mineral fraction from the ceramic mass with EDS spectrum for: a) quartz, b) albite

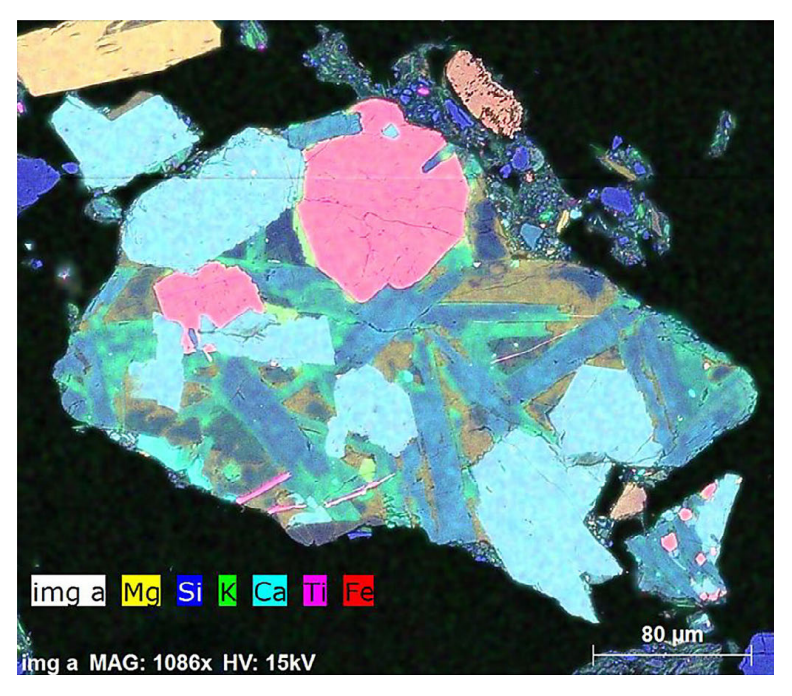


Figure 8. BSE images with elemental map of basalt in the mass for clay tile production

abrasive fraction, which has a significant effect on the intensification of wear in working elements during the extruding process.

In addition, one of the analyzed fractions was subjected to qualitative analysis of elemental composition by X-ray energy dispersive spectroscopy (EDS), the results of which are presented in Figure 9.

Within the analyzed fragment, the presence of elements such as aluminum (Al), silicon (Si),

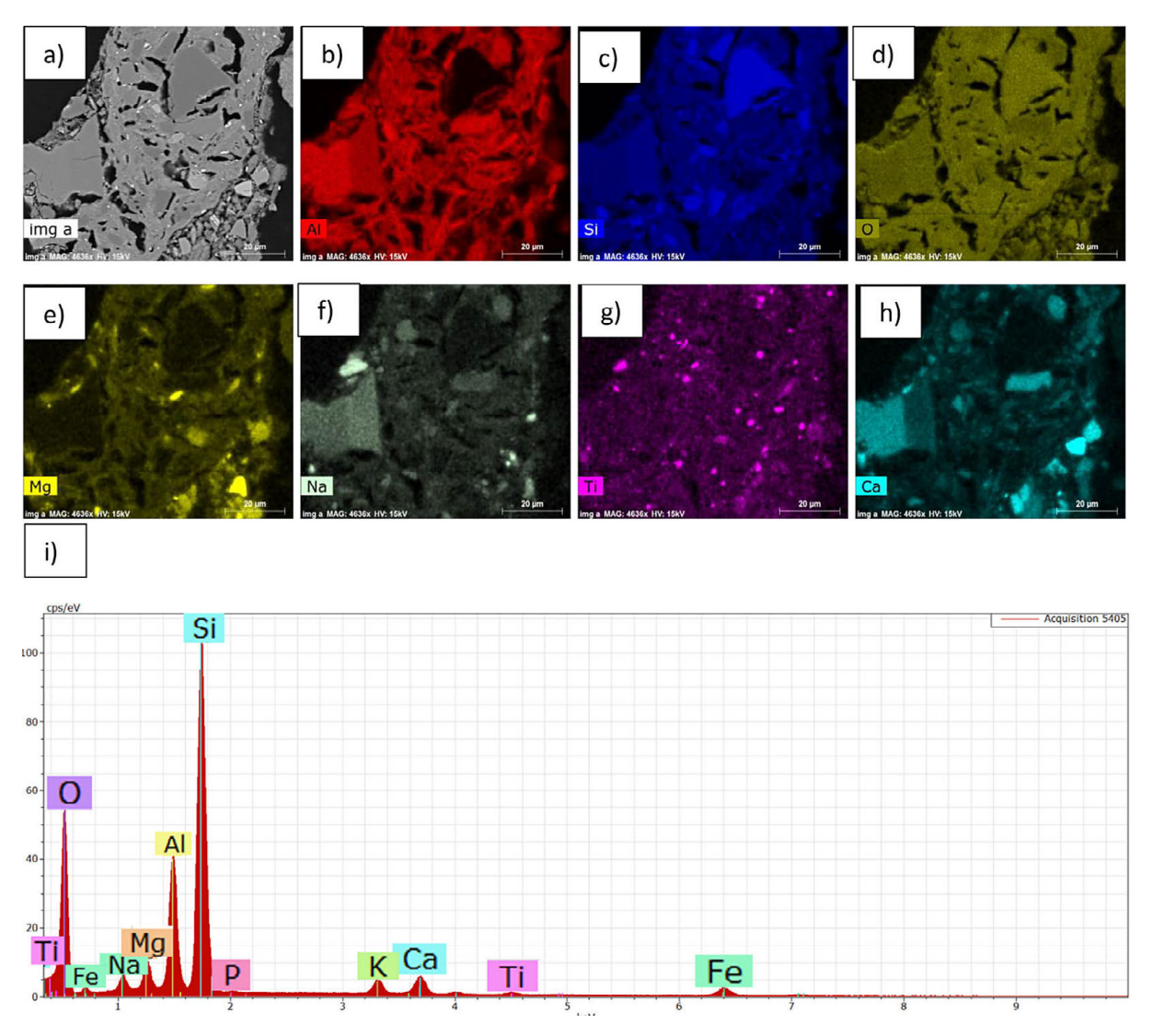


Figure 9. SEM/EDS microscopic image – (a) ceramic fragment with distribution of: b) aluminum, c) silicon, d) oxygen, e) magnesium, f) sodium, g) titanium, h) sodium, i) EDS spectrum

magnesium (Mg), and calcium (Ca) was identified, with their signals showing relatively high intensity compared to other detected elements. This chemical composition is characteristic of ceramic materials. The identified ceramic fragment within the clay body indicates that recycled powder from production waste (defective ceramic roof tiles) is added to the mix. In modern ceramic manufacturing, such material is commonly used as a non-plastic additive. This component also contributes significantly to the abrasive wear of forming tools during the extrusion process.

Thermogravimetric analysis (TGA)

The collected samples of the ceramic body used for roof tile production were subjected to thermogravimetric analysis (TGA). The

temperature range was 25–700 °C, with a heating rate of 10 °C/min. The tests were conducted in a nitrogen atmosphere (30 ml/min). Measurements were performed on two samples taken directly from the production line at different time intervals. The obtained results are presented in the graph in Figure 10 and in Table 1.

The TGA analysis of samples 1 and 2 showed a total mass loss of approximately 5.3% (5.36% for sample 1 and 5.24% for sample 2). This indicates the presence of not only clay minerals (such as vermiculite), but also mica group minerals (muscovite, biotite), which is consistent with the results of SEM-EDS analyses. Despite the time interval between sample collections, the TGA results are comparable, indicating that the ceramic body parameters in the production process are

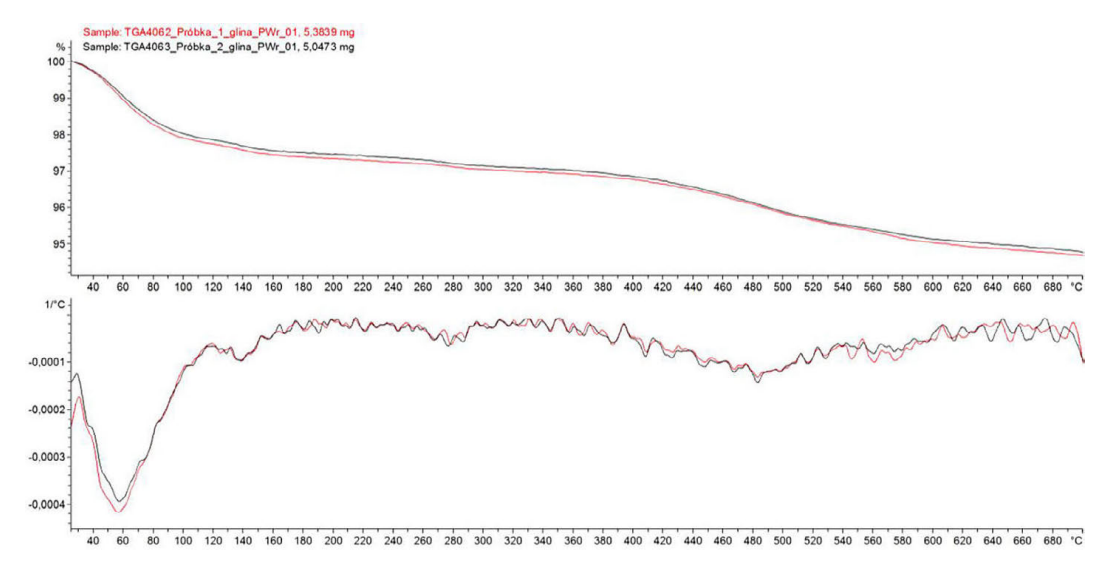


Figure 10. Summary of TG/DTG thermograms for tested samples

Table 1. Thermal parameters determined in the TG test (Δm – mass loss during TG measurement, T_{DTG} – temperature of maximum degradation rate)

Sample	∆m₁ [%]	Δm ₂ [%]	Δm ₃ [%]	Δm₄ [%]	Δm _。 [%]	T _{DTG1} [°C]	T _{DTG2} [°C]	T _{DTG3} [°C]	T _{DTG4} [°C]	T _{DTG5} [°C]
Sample 1	2.30	0.40	0.40	2.26	5.36	57	138	279	483	561
Sample 2	2.16	0.39	0.42	2.27	5.24	57	139	277	483	560

consistent and reproducible. As can be observed, the greatest mass loss occurs at around 50 °C, which corresponds to the temperature reached during the extrusion process. This highlights the importance of temperature stabilization during extrusion, as uncontrolled temperature rise may lead to premature drying of the formed material. The remaining verified temperature range provides insight into how a tile made from the analyzed clay body will behave during the subsequent thermal treatment stages: drying and firing.

Numerical modeling

The optimization of ceramic roof tile forming tools should be carried out both in the area of material selection and verification of design solutions. The most effective method for analyzing design modifications is numerical modeling. This approach enables the verification and definition of parameters whose values are difficult to measure directly during the process. In addition, numerical simulation provides preliminary insights into which solutions are most effective under operating conditions.

From the numerous research works carried out by the authors, it appears that in modeling the process of extruding the mass for the production of ceramic tiles, the most suitable approach is the meshfree method SPH. This method does not require a space mesh for calculations. This allows simulation with large deformations that occur during the extrusion of the band. For the analysis, a system was used in which the mass transport through the screws was replaced by a pusher, allowing the feedstock to move inside the forming tool set, where it is shaped. The pusher and forming tool set were prepared as dicrete rigid tools. This approach allows the computational domain to be limited to the area most relevant to the research being conducted. In addition, the number of extrusions has been reduced to only one exit, as this is allowed by the symmetry of the layout. This is shown in Figure 11.

Using numericl modeling, analyses were performed on the effects of changes in tool design on the analyzed parameters. The starting point was a standard tool configuration used for the preliminary forming of ceramic roof tiles (Figure 12a). The effect of modifying the edges of the tool on which the extruded material presses during

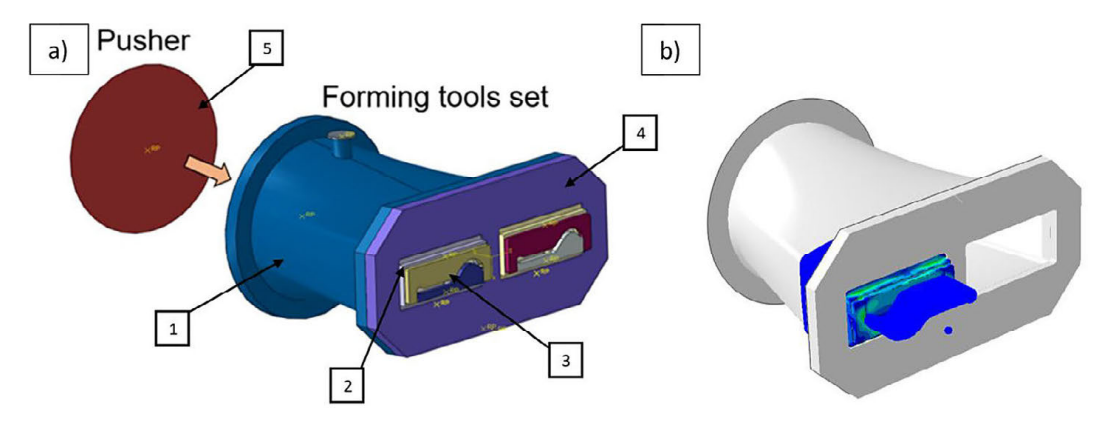


Figure 11. Numerical simulation: a) schematic diagram: 1-pressre head, 2-nozzle, 3-forming tool 4- assembling plate, 5-pusher, b) CAD models imported into the software

extrusion was verified. A solution with an introduced radius R of rounding of the working edges of the upper and lower input tool of 2.5 mm (Figure 12b) and 5mm (Figure 12c) was selected for verification. Another modification was the angle between the working surface of the upper tool and the working surface of the lower tool, which was set at 12° (Figure 12b,c).

The prepared 3D models of the three design variants of the forming tools were imported into ABAQUS software in which simulations were performed. The displacement of forming tools at all degrees of freedom was blocked, and a boundary condition was applied to the pusher for displacement along the extrusion direction. The Drucker-Prager (DP) constitutive model was used to characterize the forming material. This model is commonly applied in the analysis of granular materials such as soils, which exhibit pressuredependent plasticity - that is, their strength increases with increasing pressure. The degree of discretization of the finite element mesh was verified in terms of the quality of the results obtained. The results for the various forming tool design solutions are shown in Figure 13.

Figure 13 presents the stress distribution in the forming tool during the shaping process. As shown, the stress values obtained from the numerical simulation are not uniform and vary depending on the region of the tool. The implemented design modifications effectively reduced the areas of maximum stress concentration, as seen in the stress distribution shown in Figure 13a. High stress levels occur only locally, such as in the region depicted in Figure 13b, where stress concentration is observed in the absence of an applied rounding radius R. In contrast, the

detailed results in Figure 13c clearly show a reduction in stress levels due to the introduction of edge radii at the location where the forming material presses the tool.

Numerical simulation also allows for tracking how stresses change in different regions of the forming tools throughout the analyzed phase of the process. The area where stress concentration occurs is shown in Figure 14.

The graph presented in Figure 15 illustrates the observations previously noted in the stress distribution results. In the analyzed region, stress levels increase with the introduction of the rounding radius R. In this case, the specific value of the radius – whether 2.5 mm or 5 mm – has little influence, as the corresponding curves are very similar. During the analyzed time interval, the maximum stress reaches 400 MPa. Only the curve obtained for the tool without a radius and without an angle between the tool surfaces shows lower stress values.

Stress behavior is different in the so-called 'wave' region, which is also shown in Figure 15.

In this area, the curves overlap regardless of the tool design variant during the analyzed time interval. It is also evident that high stress levels do not occur in this area; the stress distribution is uniform and stable. In the verified period for all variants, an increasing trend of stress values can be seen regardless of the changes made.

Analysis of the operation of forming tools

During the operational tests, attention was focused on the analysis of the lower tools. These tools are adjusted less frequently during the process, which makes their wear a more reliable indicator for assessing the tested materials.

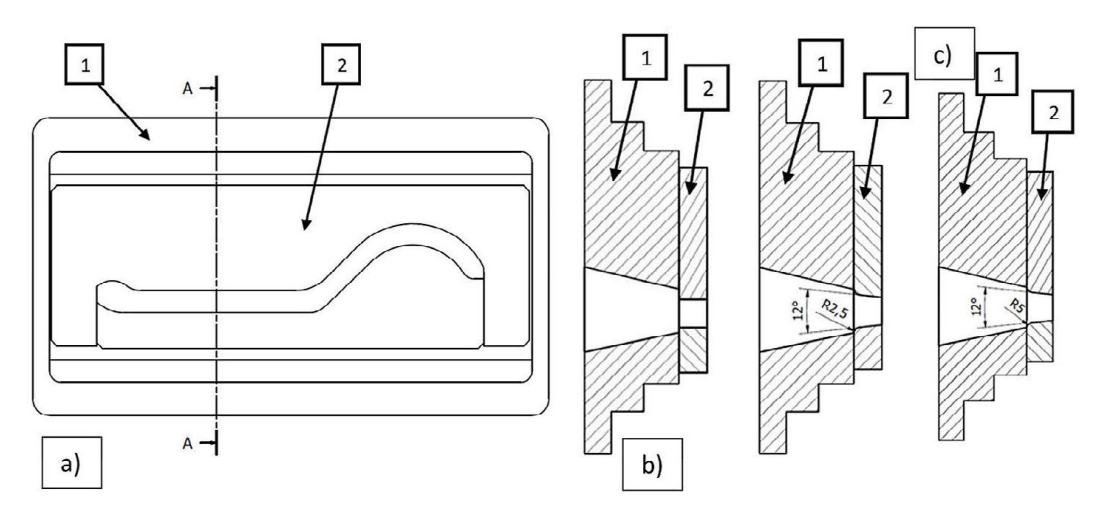


Figure 12. Modification of the design solution of the forming tool (1-nozzle, 2-forming tool): a) standrad, b) radius R = 2.5 mm, c) radius R = 5 mm

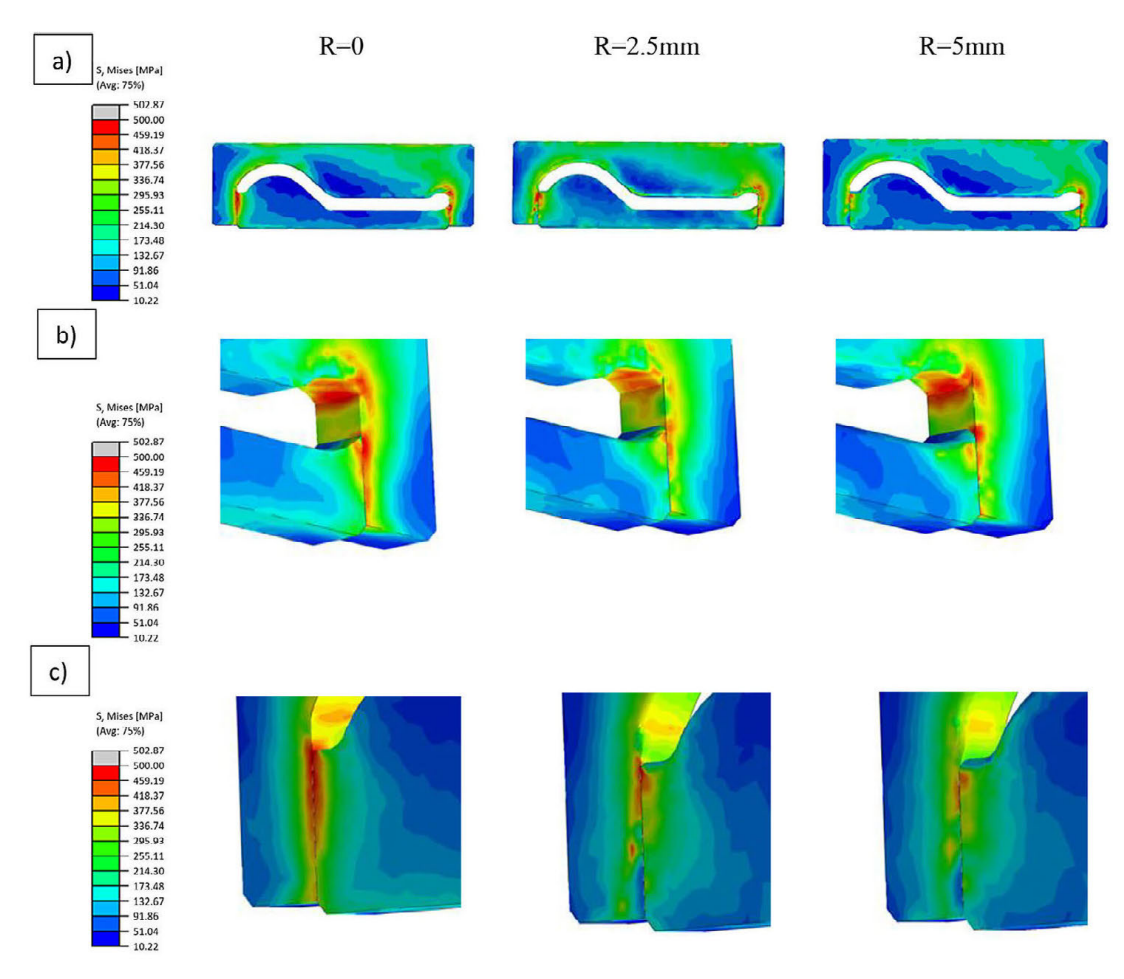


Figure 13. Results of numerical simulation of extrusion of a strand of equivalent stress distribution (von Misses): a) whole tool, b) tool area 1, c) tool area 2

As a first step, 3D scanning was performed on a new tool manufactured by CNC machining based on a CAD model. The results of this scan are shown in Figure 16. This allowed verification of the manufacturing accuracy of tools used for forming ceramic roof tiles.

The scanned forming tool, after machining and hardening, shows deviations from the CAD

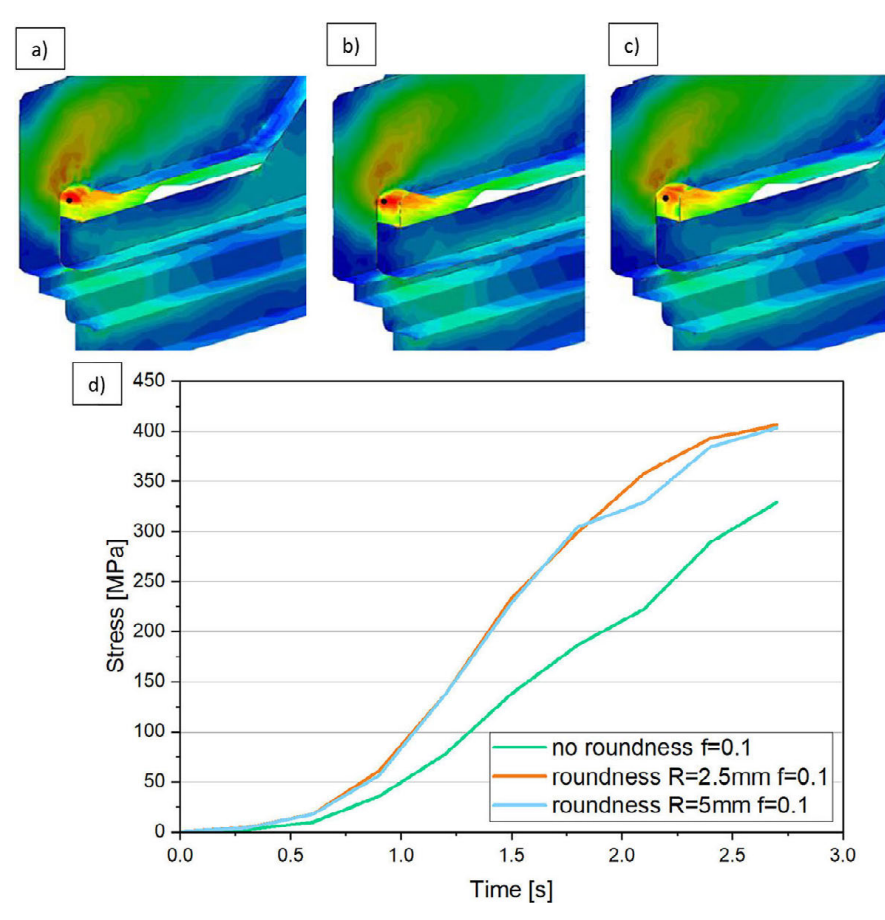


Figure 14. Comparison of results of numerical simulation of extrusion of a strand of equivalent tress distribution (von Misses): a) no radius, b) radius R = 2.5 mm, c) radius R = 5 mm, d) graph of stress changes during the analyzed process

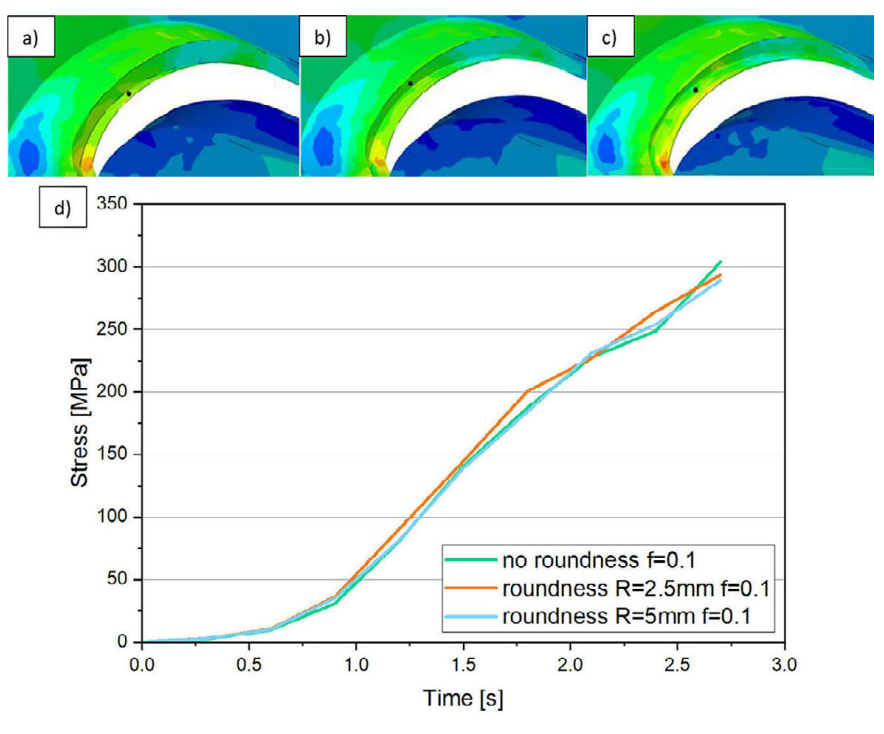


Figure 15. Comparison of results of numerical simulation of extrusion of a band of equivalent stress distribution (von Misses) for the area of the so-called "wave": a) without radius, b) radius R = 2.5 mm, c) radius R = 5 mm, d) graph of stress changes during the analyzed process

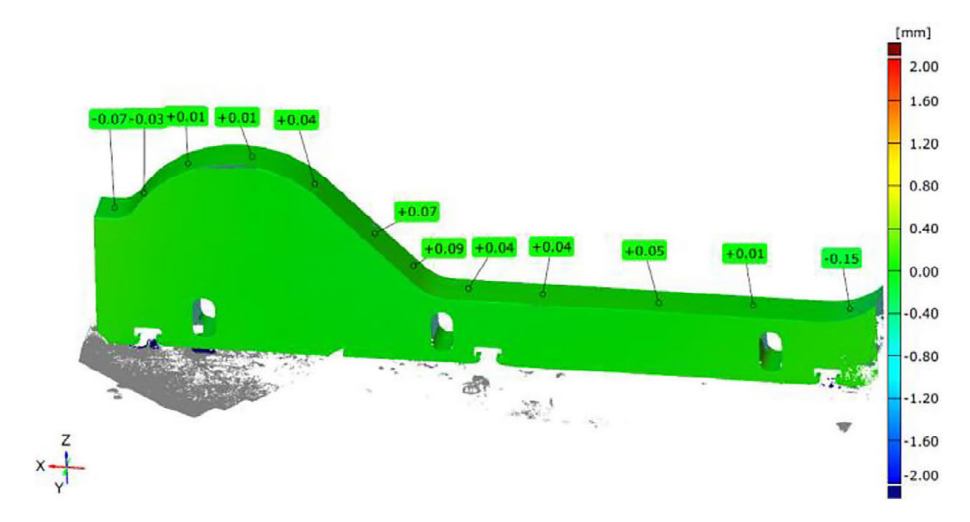


Figure 16. Scanning result of the new forming tool

model ranging from -0.15 mm to +0.09 mm. The new forming tool was manufactured with sufficient accuracy for the strand forming process, and the observed dimensional differences will not result in defects in the produced ceramic roof tiles.

To evaluate different heat treatment variants of NC11LV steel, tests were conducted under real operating conditions. Operational tests of forming tools were carried out on a two-lane screw press during standard industrial production of ceramic roof tiles. The press used in the tests operated at an extrusion pressure of 2.0–2.1 MPa,

corresponding to an average strand speed of approximately 20 m/min. For each tool variant, the aim was to carry out tests over approximately 170 hours of operation (Figure 17).

An analysis of the operational test results indicates that the lowest wear was observed in the tool made of NC11LV tool steel hardened at 1020 °C and tempered at 200 °C. For this tool, the wear of the working surface ranged from 0.68 to 1.24 mm. The other two tools exhibited higher levels of wear. The forming tool hardened at 960 °C and tempered at 450 °C showed wear in the range of 1.34 to 1.76 mm. In comparison, the

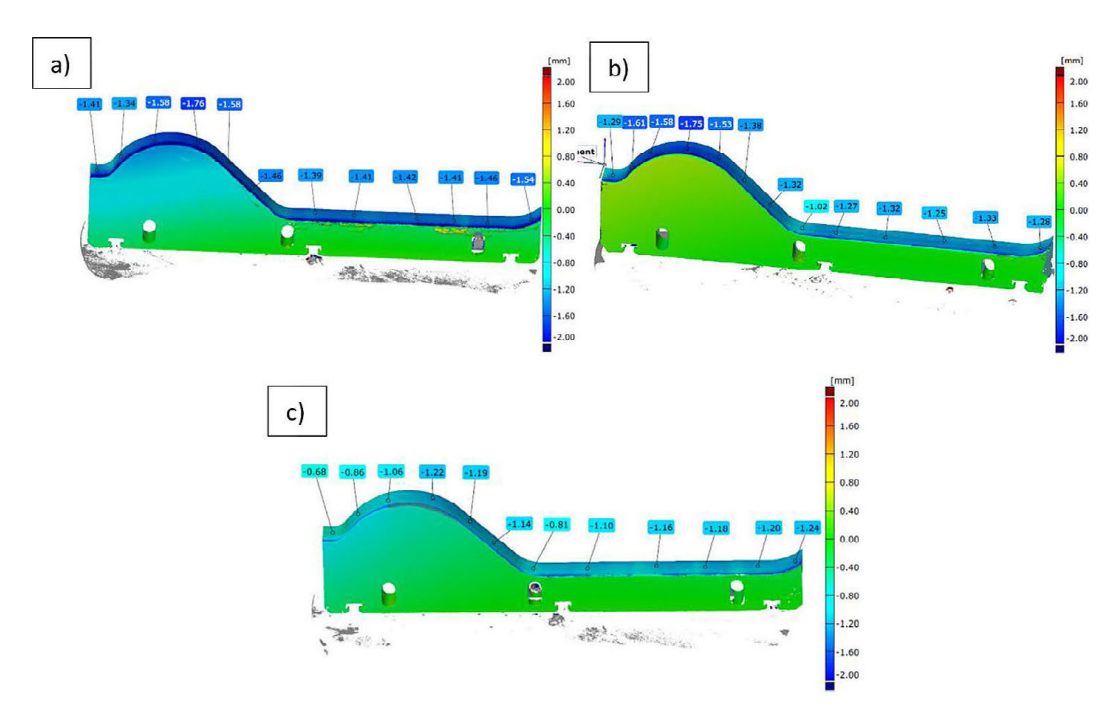


Figure 17. Scanning results of the lower forming tools: a) 960/450, b) 1060/450, c) 1020/200

tool hardened at 1060 $^{\circ}$ C and tempered at 450 $^{\circ}$ C showed wear ranging from 1.02 to 1.75 mm.

Dry abrasion test

Recently, cold-work tool steels have become increasingly popular as materials for forming tools used in ceramic roof tile production, gradually replacing wear-resistant Hardox steels. Tool steel NC11LV has proven to be particularly effective in this application. However, to meet operational performance requirements, an appropriate heat treatment must be selected. As a first step, all selected heat treatment variants were subjected to dry abrasive tests, during which the mass loss of the samples was measured and the relative wear resistance coefficient Kb was determined using the following formula:

$$K_b = \frac{Z_{ww} \cdot \rho_b \cdot N_b}{Z_{wb} \cdot \rho_w \cdot N_w} \tag{1}$$

where: Z_{ww} _ weight loss of the reference sample (g), Z_{wb} _ weight loss of the tested material (g), ρ_w _ density of the reference material, ρ_b _ density of the tested material, N_w _ number of rotations of the reference sample's friction path, N_b _ number of rotations of the tested sample's friction path.

Due to the hardness of the tested materials, the abrasion time in the conducted trials was 30 minutes, corresponding to 1800 revolutions. The reference sample was, according to the standard, C45 steel, which was tested at 600 rotations of the roll. Its average wear amounted to 0.062 g. The obtained results are presented in Table 2 and graphically in Figure 18.

The results of abrasion resistance tests conducted using the T-07 tester show that the NC11LV 1020/200 sample demonstrated the highest abrasion resistance, achieving a relative resistance coefficient of 1.610. A slightly lower value of 1.599 was obtained for the NC11LV 1060/450 sample. The greatest wear was observed for the NC11LV 960/450 sample, with a wear coefficient (Kb) of

1.371. The results obtained from the dry abrasion test of NC11LV steel show that indicate that better wear resistance parameters than in the case of the wear-resistant Hardox steels. This can be precisely verified by comparing with the results reported in the literature. For Hardox 500, the Kb coefficient does not exceed 1.200, while for Hardox Extreme in the as-delivered condition it is approximately 1.300 [27, 28].

Analysis of wear mechanisms

To illustrate the wear mechanisms occurring during the band forming process, photographs of the working surfaces of the analyzed tools were taken. The surfaces shown in Figure 19, obtained through macroscopic examination, reflect the extent of tool degradation after 170 hours of operation. In general, the macroscopically examined parts showed a similar wear mechanism regardless of the heat treatment carried out. It was observed that the wear process had a heterogeneous character. The working surfaces are dominated by clear, regular irregularities with gouge characteristics, arranged perpendicular to the direction of movement of the molded material. In the raised areas formed by this process, signs of corrosion were observed, likely developing after the tools had been withdrawn from service. This indicates significant surface degradation in this area and the mechanical removal, during the band extrusion process, of the oxide layer that forms on the steel surface due to the presence of chromium in its chemical composition. Material degradation in the raised areas is also associated with the development of high contact pressures in this region. The occurrence of more severe mechanical damage in this area is illustrated, for example, by the stereoscopic image shown in Figure 19c. It clearly shows that these areas are accompanied by surface scratching, which leads to increased roughness. In the regions where the cross-section of the tool changes, surface scratches were frequently observed, most likely caused by the movement of hard particles across the tool surface along with

Table 2. Dry abrasive test results for the tested materials

Sample NC111V	Mass I	oss Z [g] in subseque	7 [~]	K	
Sample NC11LV	1	2	3	Z _{śr} [g]	Γ _b
960/450	0.128	0.130	0.136	0.132	1.371
1060/45	0.122	0.107	0.110	0.113	1.599
1020/200	0.112	0.113	0.111	0.112	1.610

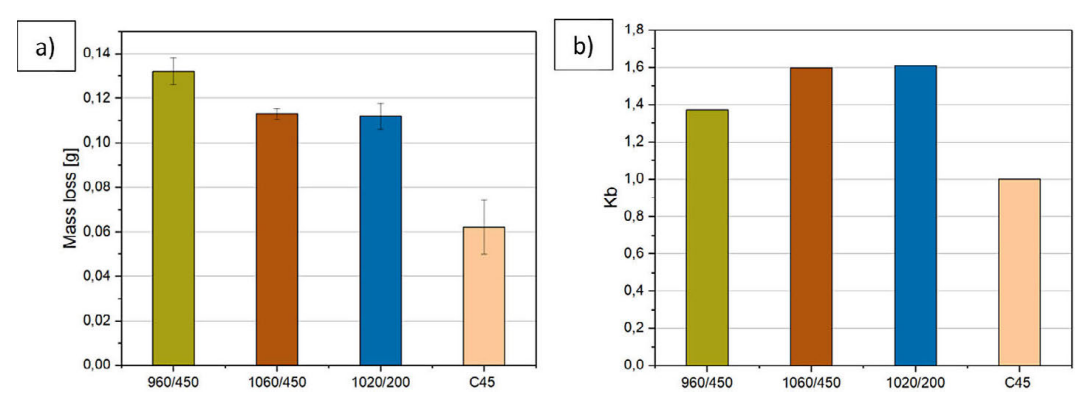


Figure 18. Dry abrasive test results: a) mass loss- average value [g], b) relative abrasive wear resistance Kb

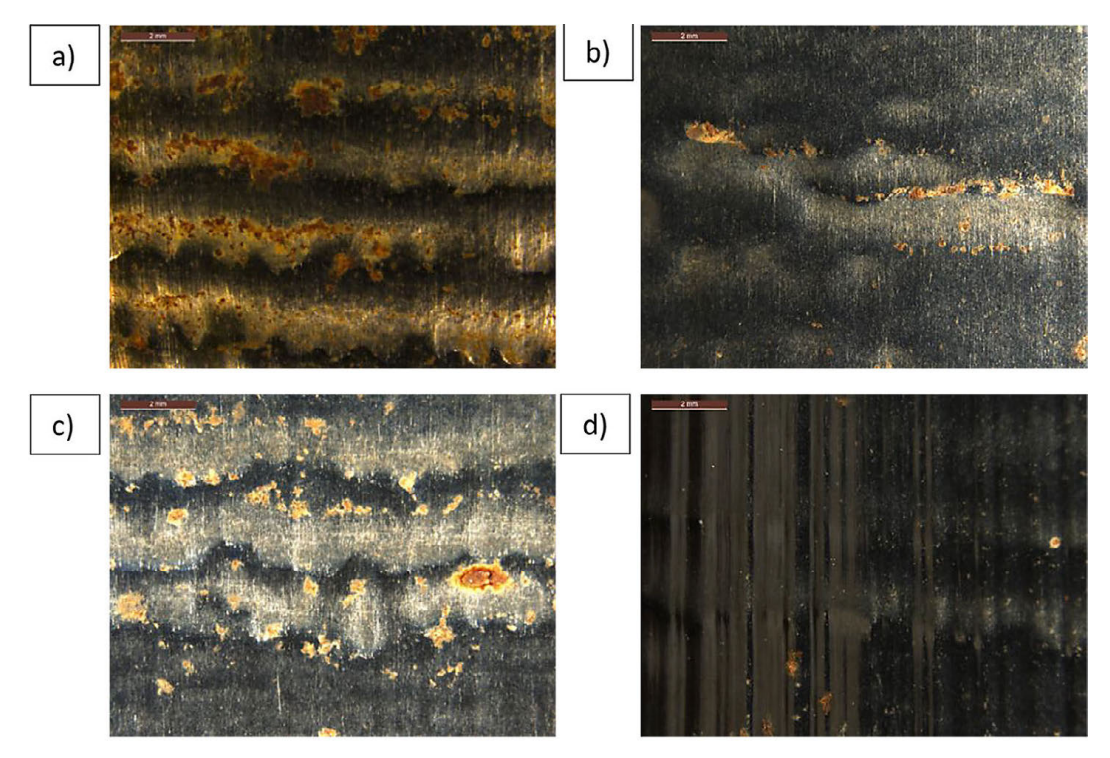


Figure 19. Tool working surface: a) 1020/200 stereoscopic microscopy, b) 960/450 stereoscopic microscopy, c) 1060/450 stereoscopic microscopy, d) 1060/450 stereoscopic microscopy

the tile material mass. These particles may include basalt fragments, identified in SEM studies of the tile material. The change in cross-section promoted the accumulation of hard particles in the analyzed area.

Particularly intense unevenness can be seen on the tool version 1020/200 (Figure 19a) and 1060/450 (Figure 19c). Surface scratches formed in the direction of material flow during extrusion are less distinct, with clearly visible scratches on the working surface identified only in Figure 19d. For all applied heat treatment parameters, the observed scratches do not constitute critical defects that would affect the quality of the formed band.

In selected areas of the tool surface, traces of adherence of the processed material (roof tile mass) were observed, especially in locations where topographic irregularities had previously been identified. Local accumulation of material may promote the intensification of tribological processes, leading to increased wear in these zones.

Microscopic examinations were also performed on the cross-section of the tool in three selected areas. Representative results of the conducted analyses are presented in Figure 20. Since all analyses were carried out on a single steel grade – NC11LV – the results obtained for the various heat treatment variants (Figure 20a–f) revealed a



Figure 20. Microstructure of NC11LV steel in the near-surface region of the friction edge – light microscopy, etched state: a),b) 1020/200, c),d) 960/450, e),f) 1060/450

microstructure typical for this material. The presence of tempered martensite with visible primary carbide precipitates was observed. On the working surface of the tool, features characteristic of abrasive wear were identified. The overall microstructure of the examined tools was similar, and no significant differences were observed between the individual samples. It should be noted that the applied heat treatment leads to subtle changes in the microstructure, primarily related to the chemical composition and the size of secondary carbide precipitates formed during tempering, as well as the presence of retained austenite in the material tempered at lower temperatures.

However, the microscopic examination did not reveal any changes in the subsurface layer that would indicate secondary tempering or the occurrence of plastic deformation, which is attributed to the low temperature of the formed material. Observations at higher magnifications indicate that more intensive wear primarily affected the matrix of the material, due to its lower hardness. As a result, the carbide precipitates were removed only secondarily, suggesting their higher resistance to mechanical factors. Hard carbide particles entering the friction zone act as a third body, promoting scratching of the tool surface.

The outer surface was also examined using a scanning electron microscope (SEM). Observations focused on the central part of the tool as well as the edge where the formed material band exits the tool. This area exhibited the most intensive tool wear, as shown in Figure 21. Observations conducted in the central region of the tool

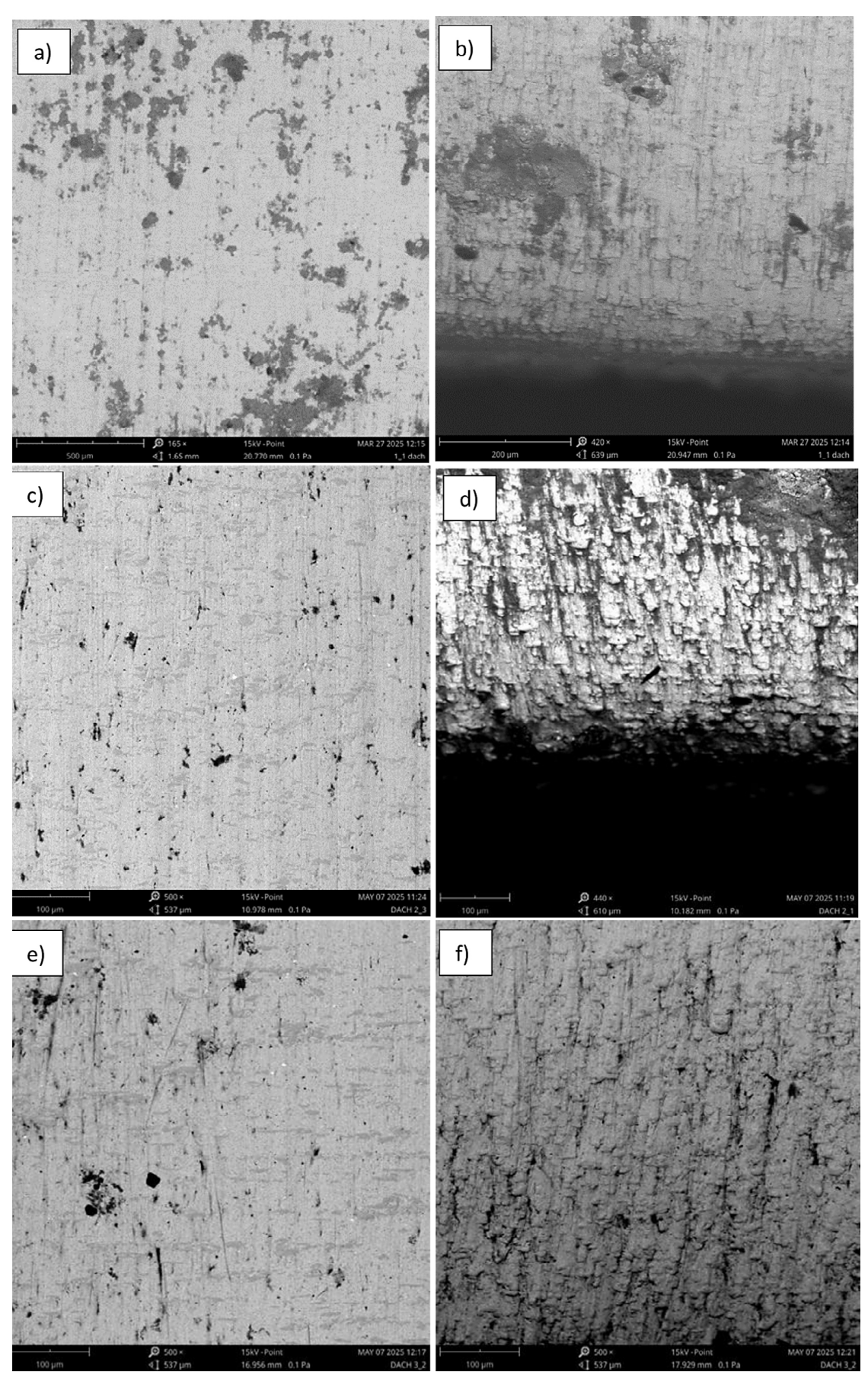
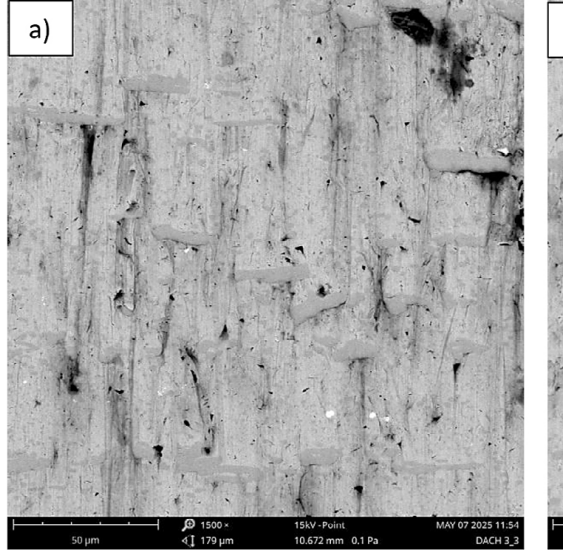


Figure 21. SEM microscopic image: a)1020/200 tool center section, b) 1020/200 tool edge, c) 960/450 tool center section, d) 960/450 tool edge, e) 1060/450 tool center section, f) 1060/450 tool edge

confirmed the findings of previous stereoscopic analyses. For all three heat treatment variants, characteristic surface scratching was observed (Figure 21a, c, e). Remnants of the processed material (roof tile mass) were also visible in the analyzed areas, indicating partial adhesion to the tool's working surface. The most significant morphological changes were found at the tool's edge, where a noticeable reduction in height was observed, suggesting intensive loading and localized wear in this region. The tool edge was also the area where the most noticeable differences between the analyzed heat treatment variants were observed. In the case of the tool subjected to heat treatment under the 960/450 variant (Figure 21d), SEM analysis revealed pronounced wear marks and intense surface scratching, indicating lower wear resistance for this variant. This can be attributed to the lowest material hardness resulting from this heat treatment, as confirmed by the hardness measurements presented in the following section. Tempering at a lower temperature leads to higher hardness in the matrix, resulting in improved resistance to tribological wear. In contrast, the reduced hardness of the material tempered at a higher temperature is primarily due to softening of the matrix, as the fraction of primary carbides remains unchanged. These carbides possess high melting points and, therefore, do not dissolve during austenitization. Consequently, matrix hardness is the key factor influencing the material's resistance to abrasive wear. By comparing the obtained results of the microstructural analysis, it

can be stated that they are consistent with the data reported in the literature. The dominant precipitates in all examined variants of heat treatment are coarser primary M_7C_3 carbides formed during solidification. In addition, finer $M_{23}C_6$ carbides can be observed, which originate from secondary precipitation during the spheroidization process of carbides, formed as a result of the transformation of austenite into ferrite—carbide microstructures during cooling. Literature data indicate that during prolonged annealing, M_7C_3 carbides may transform into $M_{23}C_6$ carbides through diffusion [25, 29, 30].

SEM observations conducted at high magnifications show that the irregularities identified during macroscopic analysis are the result of uneven material wear, caused by variations in the hardness of the structural components present in the material's microstructure. A representative microscopic image is shown in Figure 22. It can be observed that the movement of the roof tile mass leads to surface scratching and grooving, which are halted by carbide precipitates. This likely causes a change in the material flow direction, resulting in a macroscopically visible area with reduced degradation further along the surface. At the microscopic level, increased wear of the matrix is observed immediately behind the carbide precipitates, as shown in Figure 23. This type of wear leads to the formation of "fish scale"-like patterns, which were observed at the tool edge. This indicates that the wear mechanism at the edge does not differ from that in the



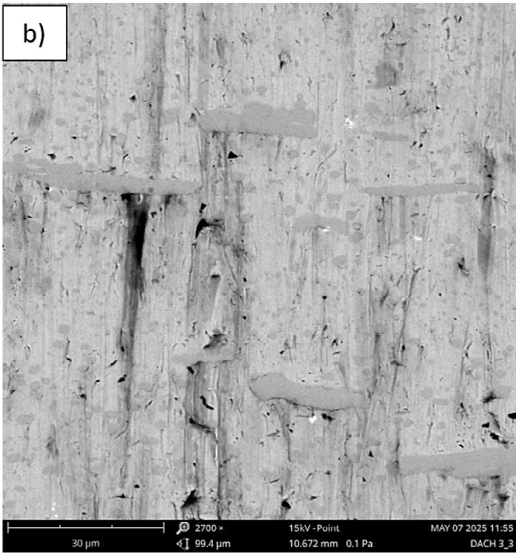


Figure 22. Uneven wear of material structure components, a) Fragment of the surface area of sample 1060/450, b) Magnified section of the area from figure a. SEM

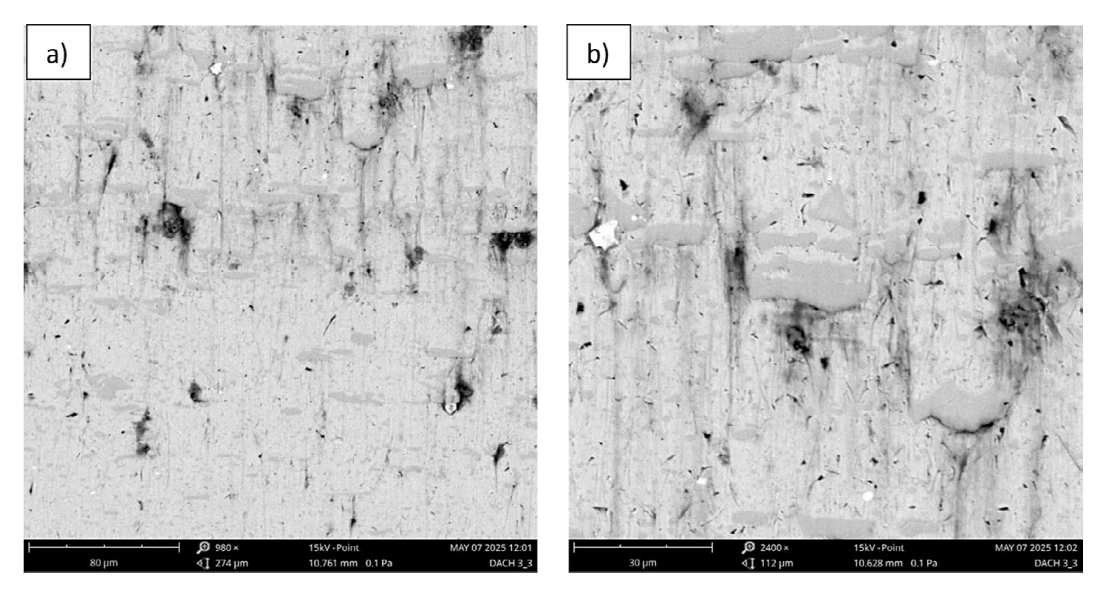


Figure 23. Uneven wear of material structure components, (a) Fragment of the surface area of sample 1060/450, (b) Magnified section of the area from figure a. SEM

central part of the tool, although its intensity is significantly higher.

Hardness measurement

In order to further analyze the properties of the tested materials, hardness measurements were performed using the Vickers method for each heat treatment variant of NC11LV steel. The measurement started from the edge of the tool forming a band of ceramic mass, up to a distance of 10mm. In order to obtain the most reliable results, measurements were made at 10

points with a load of 1 kg (HV1). The graphs shown in Figure 24 summarize the results of the hardness measurements.

Analysis of the hardness measurement results revealed a clear variation depending on the applied heat treatment variant. The highest hardness values were recorded for the sample taken from the forming tool subjected to heat treatment in the 1020/200 variant, where hardness ranged between 750–800 HV1. In contrast, the lowest values around 580 HV1 were observed for the 960/450 sample, with this level maintained across most of the analyzed

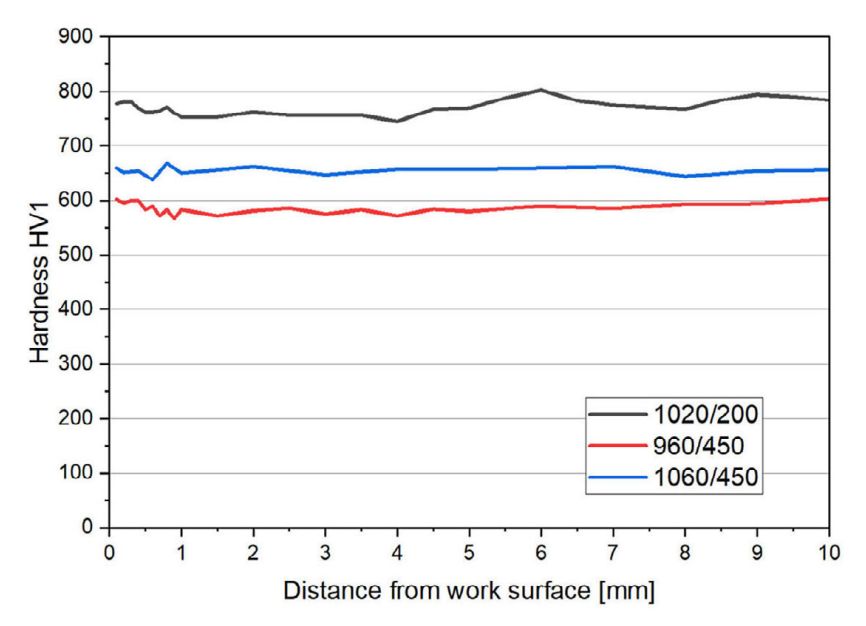


Figure 24. Results of hardness measurements for the analyzed forming tool materials

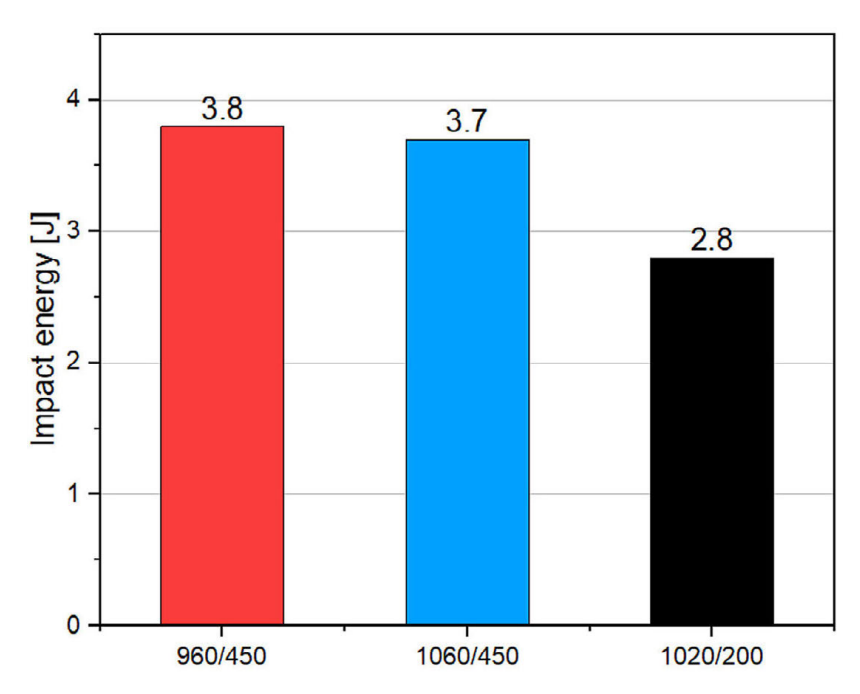


Figure 25. Charpy V-notch test results for the analyzed forming tool materials

cross-section. Intermediate values (650–670 HV1) were recorded for the sample heat-treated in the 1060/450 variant.

Based on these results, it can be concluded that the highest hardness was obtained for the sample taken from the tool that exhibited the lowest operational wear. This indicates a significant correlation between the hardness of the tool material and its wear resistance. Therefore, the higher hardness of the forming tool material may result in longer tool life under real operating conditions.

Impact strength test

The second mechanical parameter examined in the conducted research was impact toughness. The tests were carried out using a Charpy V-notch (CVN) tester. The impact toughness measurements were performed at a temperature of 50 °C, corresponding to the operating temperature of the tool during ceramic mass extrusion. The obtained results are presented in Figure 25.

The obtained results show that the hardened tool steel NC11LV, regardless of the applied heat treatment, is characterized by low ductility. The heat treatment parameters have only a slight influence on impact toughness. Only for the sample 1020/200 is the CVN value minimally lower than in the other samples, amounting to 2.8 J. This corresponds with the hardness of this sample, which for 1020/200 is the highest (750–800 HV1). For the other two samples,

the impact toughness remained at a comparable level, amounting to 3.8 J for sample 960/450 and 3.7 J for sample 1060/450.

When analyzing the industrial application of forming tools for ceramic roof tiles, impact toughness plays a secondary role. During operation, the tools are mainly subjected to continuous loads resulting from the pressure of the extruded mass, while potential impact loads may only occur during assembly or adjustment.

CONCLUSIONS

This paper presents the results of comprehensive operational studies on tools used in the forming of ceramic mass for roof tile production, with a particular focus on abrasive wear mechanisms. The main factors influencing tool degradation were identified, including the presence of hard mineral components (e.g. quartz, basalt, albite) and high mechanical loads arising from process parameters. The effectiveness of appropriately selected heat treatment parameters for NC11LV steel in increasing tool wear resistance was demonstrated. Laboratory and industrial tests confirmed favorable mechanical properties achieved through these treatments, combining high hardness with resistance to brittle fracture. For a more detailed analysis of the process, the advanced numerical method SPH (smoothed particle hydrodynamics) was used to model the flow of the ceramic mass, taking into account the presence of abrasive fractions. The obtained results are an important contribution to the development of tools for intensive ceramic extruding processes and to the optimization of their service life. Such a study carried out allowed to come to the following conclusions:

The reason for the intensive abrasive wear of forming tools in this process is the specific nature of the material being formed. Based on the analysis of the chemical and mineralogical composition, it was possible to identify numerous hard fractions that indicate the abrasive nature of the mass for the manufacture of ceramic tiles. These primarily include quartz (SiO₂) with a Mohs hardness of≈7, basalt containing hard silicate minerals, and albite (NaAlSi₃O₃) also of high hardness. An additional abrasion-enhancing component is ceramic, added to the mass in the form of recycled flours from defective products, containing particles ranging in size from 10 to 150 µm and high hardness (up to 8 on the Mohs scale).

Also important for tool wear during band forming are operating conditions, which are affected by process parameters. Among the most significant is the extrusion pressure, which oscillates at 2.1 MPa during the industrial process. Also verified was the temperature of the mass at the time of forming, which fluctuates between 43–47 °C, which promotes partial plasticization of the mass, but does not eliminate the effects of strong friction and adhesion.

Under laboratory conditions, a variant of NC11LV steel quenched at 1020 °C and tempered at 200 °C for 2 hours showed the lowest weight loss in a dry abrasive wear test (test using No. 90 electrocorundum abrasive). It was characterized by a relative abrasive wear resistance Kb of 1.610. This was then also confirmed in in-service tests, where the tool heat-treated according to these parameters showed the lowest degree of surface wear after 170 hours of operation - the thickness loss of the working surface was about 0.12 mm (the average value for five micrometer measurements).

Under laboratory conditions in the dry abrasion test, the lowest weight loss was observed in the NC11LV steel variant quenched at 1020 °C and tempered at 200 °C for 2 hours. This was then also confirmed in in-service tests, where the tool heat-treated according to these parameters also wore the least.

Examination of the NC11LV steel after heat treatment revealed a stable microstructure, consisting of tempered martensite and numerous, fine, evenly distributed carbides of chromium and vanadium. No changes indicating structural degradation or plastic deformation were observed in the surface layer. Macroscopic analysis of the working surfaces of the tools after 170 hours of operation showed dominant regular deformations up to 30-40 µm deep, perpendicular to the direction of movement of the formed material. Local traces of adhesion of ceramic mass were also registered, especially in the band entrance zone, which can lead to uneven wear, but the observed scratches and micro-scratches do not significantly affect the quality of the formed band (dimensional deviations did not exceed ± 0.3 mm).

For more extensive analysis and optimization work, numerical modeling is best used. Due to the large displacements of the material, its complex composition and dynamic shape changes during flow, the SPH meshless method was considered the most effective. Based on the numerical model developed by the authors and built in Abaqus software, it is possible to verify the structural changes and geometry of the forming channel. The model consisted of more than 250,000 SPH particles representing the ceramic material and Lagrange elements mapping the tool. The ability to map stress concentration zones, flow paths and locate potential wear areas was verified.

Further development, optimizations and verifications of the developed numerical model will make it possible to simulate longer sections of the process - it is expected to be possible to model a section of the order of 500–700 mm in strand length, which will make it possible to collect much more data on the operating conditions of tools forming ceramic tiles. This will make it possible to identify the most stressed areas of the tools, assess the effects of design changes, and support processes regarding material selection and surface treatment.

The applied heat treatment of NC11LV tool steel affects the durability of tools used for forming ceramic roof tiles in the extrusion process. In the analyzed industrial application, the most effective variant proved to be hardening at 1020 °C followed by tempering at 200 °C, which resulted in the highest hardness. This significantly reduces the need for tool replacement during operation. At the same time, a high quality of the formed strand is ensured, which directly translates into

the quality of the final products. The results demonstrate a strong potential for the use of this steel in forming elements for various types of ceramic products, such as roof tiles, bricks, and tiles. Moreover, the incorporation of numerical modeling into the design of forming tools represents an innovative approach to research and development in the ceramic industry, which significantly contributes to a deeper understanding of the phenomena occurring during ceramic forming.

REFERENCES

- Quinteiro P, Almeida MI, Serra J, et al. Life cycle assessment of ceramic roof tiles: A temporal perspective. Journal of Cleaner Production 2022;363:132568. https://doi.org/10.1016/j. jclepro.2022.132568
- Mezquita A, Monfort E, Ferrer S, Gabaldón-Estevan D. How to reduce energy and water consumption in the preparation of raw materials for ceramic tile manufacturing: Dry versus wet route. Journal of Cleaner Production 2017;168:1566–1570. https:// doi.org/10.1016/j.jclepro.2017.04.082
- 3. Javed S, Conte S, Molinari C, et al. Strategies and pathways to improve circularity in ceramic tile production. Journal of Cleaner Production 2025;517:145788. https://doi.org/10.1016/j.jclepro.2025.145788
- Agrafiotis C, Tsoutsos T. Energy saving technologies in the European ceramic sector: a systematic review. Applied Thermal Engineering 2001;21:1231–1249. https://doi.org/10.1016/S1359-4311(01)00006-0
- 5. Atılgan Türkmen B, Budak Duhbacı T, Karahan Özbilen Ş. Environmental impact assessment of ceramic tile manufacturing: a case study in Turkey. Clean Techn Environ Policy 2021;23:1295–1310. https://doi.org/10.1007/s10098-021-02035-w
- 6. Powell J, Assabumrungrat S, Blackburn S. Design of ceramic paste formulations for co-extrusion. Powder Technology 2013;245:21–27. https://doi.org/10.1016/j.powtec.2013.04.017
- Dondi M, Raimondo M, Zanelli C. Clays and bodies for ceramic tiles: Reappraisal and technological classification. Applied Clay Science 2014;96:91
 109. https://doi.org/10.1016/j.clay.2014.01.013
- 8. Dubale M, Vasić MV, Goel G, et al. Utilization of construction and demolition mix waste in the fired brick production: the impact on mechanical properties. Materials 2022;16:262. https://doi.org/10.3390/ma16010262
- 9. Riaz MH, Khitab A, Ahmad S, et al. Use of ceramic waste powder for manufacturing durable and ecofriendly bricks. Asian J Civ Eng 2020;21:243–252. https://doi.org/10.1007/s42107-019-00205-2

- Reh H. Current Classification of Ceramic Materials.
 In: Händle F (ed) Extrusion in Ceramics. Springer Berlin Heidelberg, Berlin, Heidelberg, 2009;35–57.
- Mennig G. Tribological Principles. In: Händle F (ed) Extrusion in Ceramics. Springer Berlin Heidelberg, Berlin, Heidelberg, 2009;313–320.
- 12. Ligier K, Lemecha M, Napiórkowski J. The effect of abrasive mass moisture contenton the abrasion-resistant steel wear rate. Tribologia 2019;284:75–82. https://doi.org/10.5604/01.3001.0013.4152
- 13. Hawryluk M, Lachowicz MM, Marzec J, et al. Comparative analysis of the wear of NC11LV and hardox 600 steel used in tools for extrusion of clay strands in the process of producing ceramic roof tiles. Materials 2022;16:293. https://doi.org/10.3390/ma16010293
- 14. Reisinger W. Measures for Protection Against Abrasion on Screws Used in Extruding Ceramic Compounds. In: Händle F (ed) Extrusion in Ceramics. Springer Berlin Heidelberg, Berlin, Heidelberg, 2009;321–329.
- 15. Jiang J, Stack MM. Modelling sliding wear: From dry to wet environments. Wear 2006;261:954–965. https://doi.org/10.1016/j.wear.2006.03.028
- 16. Santos MB, Labiapari WS, Ardila MAN, et al. Abrasion–corrosion: New insights from force measurements. Wear 2015;332–333:1206–1214. https://doi.org/10.1016/j.wear.2015.01.002
- 17. Händle F. Wear, Tear and No End. In: The Art of Ceramic Extrusion. Springer International Publishing, Cham, 2019;113–120.
- 18. Hawryluk M, Marzec J, Lachowicz M, et al. Evaluation of the possibility of improving the durability of tools made of X153CrMoV12 steel used in the extrusion of a clay band in ceramic roof tile production. Materials Science-Poland 2023;41:94–109. https://doi.org/10.2478/msp-2023-0011
- 19. Hryniewicz T, Nykiel T. Fluctuations in chemical composition of m 7 c 3 carbides in the soft annealed Nc11lv/D2 steel. Advances in Materials Science 2014;14:24–30. https://doi.org/10.2478/adms-2014-0003
- 20. Januszewicz B, Wołowiec E, Kula P. The role of carbides in formation of surface layer on steel X153CrMoV12 due to low-pressure nitriding (Vacuum Nitriding). Met Sci Heat Treat 2015;57:32–35. https://doi.org/10.1007/s11041-015-9830-5
- 21. Kut S, Nowotyńska I. The effect of the extrusion ratio on load and die wear in the extrusion process. Materials 2022;16:84. https://doi.org/10.3390/ ma16010084
- 22. Zhang H, Li X, Deng X, et al. Numerical simulation of friction extrusion process. Journal of Materials Processing Technology 2018;253:17–26. https://doi.org/10.1016/j.jmatprotec.2017.10.053
- 23. Kocserha I, Kristály F. Effects of extruder head's

- geometry on the properties of extruded ceramic products. MSF 2010;659:499–504. https://doi.org/10.4028/www.scientific.net/MSF.659.499
- 24. Hawryluk M, Marzec J, Madej Ł, et al. A preliminary study on developing a material model based on a mixture of clay and ceramic flour intended for the extrusion of bands for ceramic roof tiles to establish a numerical model for the load on forming tools. In: Proceedings 33rd International Conference on Metallurgy and Materials 2024;105–111
- 25. Wieczerzak K, Bala P, Dziurka R, et alThe effect of temperature on the evolution of eutectic carbides and M 7 C 3 → M 23 C 6 carbides reaction in the rapidly solidified Fe-Cr-C alloy. Journal of Alloys and Compounds 2017;698:673–684. https://doi.org/10.1016/j.jallcom.2016.12.252
- Leśniewski T, Lachowicz M, Hawryluk M, Marzec J. Insight into abrasive wear of x153crmov12 tool steel microalloyed with varied niobium content. Tribologia 2025;311:17–28. https://doi.org/10.5604/01.3001.0055.0790

- 27. Szala M, Szafran M, Matijošius J, Drozd K. Abrasive wear mechanisms of S235JR, S355J2, C45, AISI 304, and hardox 500 steels tested using garnet, corundum and carborundum abrasives. Adv Sci Technol Res J 2023;17:147–160. https://doi.org/10.12913/22998624/161277
- 28. Zemlik M, Białobrzeska B, Konat Ł. The effect of grain size on the mechanical properties and abrasion resistance of high-strength Hardox Extreme steel. Adv Sci Technol Res J 2025;19:214–236. https:// doi.org/10.12913/22998624/207125
- Krbaťa M, Eckert M, Križan D, et al. Hot deformation process analysis and modelling of X153CrMoV12 steel. Metals 2019;9:1125. https://doi.org/10.3390/ met9101125
- Kondrat'ev SYu, Kraposhin VS, Anastasiadi GP, Talis AL. Experimental observation and crystallographic description of M7C3 carbide transformation in Fe-Cr-Ni-C HP type alloy. Acta Materialia 2015;100:275-281. https://doi.org/10.1016/j. actamat.2015.08.056